9-2007

Role of mitochondrial electron transport complex I in coenzyme Q1 reduction by intact pulmonary arterial endothelial cells and the effect of hyperoxia

Marilyn P. Merker
Medical College of Wisconsin

Said H. Audi
Marquette University, said.audi@marquette.edu

Brian J. Lindemer
Medical College of Wisconsin

Gary S. Krenz
Marquette University, gary.krenz@marquette.edu

Robert D. Bongard
Medical College of Wisconsin

American Journal of Physiology : Lung Cellular and Molecular Physiology, Vol. 293, No. 3 (September 2007): L809-819. DOI.

Role Of Mitochondrial Electron Transport Complex I In Coenzyme Q_1 Reduction by Intact Pulmonary Arterial Endothelial Cells and The Effect Of Hyperoxia

Marilyn P. Merker
Department of Anesthesiology, Medical College of Wisconsin, Milwaukee, WI
Department of Pharmacology and Toxicology, Medical College of Wisconsin, Milwaukee, WI
Zablocki Veterans Affairs Medical Center, Milwaukee, WI
Said H. Audi
Department of Pulmonary Medicine, Medical College of Wisconsin, Milwaukee, WI
Department of Biomedical Engineering, Marquette University, Milwaukee, WI
Zablocki Veterans Affairs Medical Center, Milwaukee, WI
Brian J. Lindemer
Department of Anesthesiology, Medical College of Wisconsin, Milwaukee, WI
Zablocki Veterans Affairs Medical College, Milwaukee, WI
Gary S. Krenz

Department of Pulmonary Medicine, Medical College of Wisconsin, Milwaukee, WI
Department of Mathematics, Statistics and Computer Science, Marquette University, Milwaukee, WI
Zablocki Veterans Affairs Medical Center, Milwaukee, WI
Robert D. Bongard
Department of Pulmonary Medicine, Medical College of Wisconsin, Milwaukee, WI
Zablocki Veterans Affairs Medical Center, Milwaukee, WI

Abstract

The objective was to determine the impact of intact normoxic and hyperoxia-exposed (95% O_2 for 48 h) bovine pulmonary arterial endothelial cells in culture on the redox status of the coenzyme Q_{10} homolog coenzyme Q_1 (CoQ_1). When CoQ_1 (50 μM) was incubated with the cells for 30 min, its concentration in the medium decreased over time, reaching a lower level for normoxic than hyperoxia-exposed cells. The decreases in CoQ_1 concentration were associated with generation of CoQ_1 hydroquinone (CoQ_1H_2), wherein 3.4 times more CoQ_1H_2 was produced in the normoxic than hyperoxia-exposed cell medium (8.2 ± 0.3 and 2.4 ± 0.4 μM, means ± SE, respectively) after 30 min. The maximum CoQ_1 reduction rate for the hyperoxia-exposed cells, measured using the cell membrane-impermeant redox indicator potassium ferricyanide, was about one-half that of normoxic cells (11.4 and 24.1 $nmol \cdot min^{-1} \cdot mg^{-1}$ cell protein, respectively). The mitochondrial electron transport complex I inhibitor rotenone decreased the CoQ_1 reduction rate by 85% in the normoxic cells and 44% in the hyperoxia-exposed cells. There was little or no inhibitory effect of NAD(P)H:quinone oxidoreductase 1 (NQO1) inhibitors on CoQ_1 reduction. Intact cell oxygen consumption rates and complex I activities in mitochondria-enriched fractions were also lower for hyperoxia-exposed than normoxic cells. The implication is that intact pulmonary endothelial cells influence the redox status of CoQ_1 via complex I-mediated reduction to CoQ_1H_2, which appears in the extracellular medium, and that the hyperoxic exposure decreases the overall CoQ_1 reduction capacity via a depression in complex I activity.

Among the metabolic functions of the pulmonary endothelium is the ability to influence the redox status and disposition of redox active compounds such as quinones via the activity of endothelial surface and/or intracellular quinone reductases, hydroquinone oxidases, and other redox processes (4, 28, 30). The size of the pulmonary endothelial surface and its position in the circulation implicate this endothelial function as a determinant in the bioactivity of various physiological, pharmacological, chemotherapeutic, xenobiotic, and dietary redox active compounds in the lung, blood, and downstream vessels and organs.

The overall impact of the pulmonary endothelium on redox active substances depends on the properties of the substances themselves (e.g., propensity to permeate cell membranes and to act as an electron acceptor for any given reductase) as well as the properties of the pulmonary endothelial cells (e.g., activities and complement of available redox enzymes). Thus, of the redox active compounds we have studied, including the quinones coenzyme Q_0 and duroquinone (DQ), and in the present study, coenzyme Q_1 (CoQ_1), the thiazine polymer (TBOP), and potassium ferricyanide [$K_3Fe(CN)_6^{3-}$], their differing physical and chemical properties influence the subcellular site of reduction, the electron donor utilized, the dominant reductase involved, and/or the effects of metabolic or prosthetic group inhibitors (4, 9, 28–32). These diverse characteristics make such compounds useful probes of redox function not only of pulmonary endothelial cells in culture but also in the intact perfused rodent lung (2, 3, 5). With regard to the properties of the cells themselves, it is well known that expression and/or activities of various pulmonary endothelial redox enzymes are influenced by pro-oxidant stimuli, with the potential outcome being a change in pulmonary endothelial metabolism of redox active compounds (10, 22, 26, 28).

These concepts are represented by the observation that when intact bovine pulmonary arterial cells were incubated with 50 μM DQ, the two-electron reduction product durohydroquinone (DQH_2) appeared in the extracellular medium, with reduction effected primarily via the ubiquitous cytosolic quinone reductase NAD(P)H:quinone oxidoreductase 1 (NQO1) (28, 30). Consistent with the fact that NQO1 is under transcriptional control of the antioxidant response element (ARE), exposure of the cells to oxidant stress (hyperoxia, 95% O_2 for 48 h) resulted in NQO1 induction, thereby doubling the capacity of the intact cells to generate extracellular DQH_2 when incubated with DQ (23, 28). Promotion of two-electron DQ reduction in the hyperoxia-exposed cells provided increased competition for semiquinone production via one-electron reduction, illustrating one of the classic protective effects of NQO1 (11). DQ was also reduced on passage through the circulation of the perfused rat lung, and exposure of rats to hyperoxia (21 days; 85% O_2) increased lung NQO1 protein, total activity, and DQ reduction capacity (5).

A question raised by these observations is whether the effect of hyperoxia to increase the DQ reduction capacity of intact pulmonary endothelial cells via NQO1 induction extends to other quinone substrates. We chose CoQ_1 for further study because it has been used as an amphipathic electron acceptor for various oxidoreductases, including NQO1, as isolated enzymes or in subcellular fractions and has nearly the same water and lipid solubility properties as DQ (8, 12, 16, 18, 33, 36). With respect to the reduction mechanism in intact cells, an NQO1 contribution to CoQ_1 hydroquinone (CoQ_1H_2) generation has been identified in rat hepatocytes and astrocytes, and the protective effect of CoQ_1 in complex I dysfunction in hepatocytes has been attributed to NQO1-mediated CoQ_1 reduction followed by CoQ_1H_2 oxidation at complex III (12). On the other hand, transplasma membrane electron transport (TPMET) has been suggested as a mechanism for CoQ_1 reduction in intact human red blood cells, Hep G cells, and chick neurons (42, 44). As a CoQ_{10} homolog, CoQ_1 is also a highly effective NADH:ubiquinone oxidoreductase (mitochondrial electron transport complex I) substrate in mitochondria or submitochondrial particles (27), but to our knowledge, a contribution of complex I to CoQ_1 reduction in intact cells has not been identified.

The goal of the present study was to determine whether CoQ_1 is reduced in the presence of bovine pulmonary arterial endothelial cells and, if so, to evaluate the redox processes involved and the effect of oxidative stress on cellular reduction capacity. The focus was on the impact of the intact cells on CoQ_1 redox status in the extracellular medium. Hyperoxia was chosen as the oxidative stress to gain further insight into its effects on quinone metabolism, wherein it was originally selected because extensive functional, molecular, and morphological studies have revealed the pulmonary endothelium to be an initial and key target of hyperoxic lung injury (14).

MATERIALS AND METHODS

CoQ_1 [2,3-dimethoxy-5-methyl-6-(3-methyl-2-butenyl)-1,4-benzoquinone], potassium hexocyanoferrate (III) [$K_3Fe(CN)_6^{3-}$, hereafter referred to as ferricyanide or $Fe(CN)_6^{3-}$], HEPES, and other reagents, unless otherwise specified, were purchased from Sigma Chemical (St. Louis, MO) or Burdick and Jackson, the latter for HPLC mobile phase reagents.

RPMI 1640 tissue culture medium and fetal calf serum were obtained from Invitrogen (Carlsbad, CA). Biosilon microcarrier beads were obtained from Nunc (Roskilde, Denmark). Protein determinations were performed using the Bio-Rad protein assay reagent (Bio-Rad Laboratories, Hercules, CA). CoQ_1H_2 was prepared by reduction of CoQ_1 with potassium borohydride as previously reported (28). The mechanism-based irreversible NQO1 inhibitor ES936 was the kind gift of Drs. David Siegel and David Roth (School of Pharmacy, University of Colorado Health Sciences Center, Denver, CO) (15). Toluidine blue O was incorporated in an acrylamide polymer by copolymerization of toluidine blue O methylacrylamide and acrylamide to prepare the toluidine blue O polyacrylamide (TBOP), as previously described (9). The amount of reducible toluidine blue O ($TBOP^+$) per unit

mass of the TBOP preparation used in the current study was ~17 nmol/mg, determined as described previously (9).

Endothelial cell culture.

Bovine pulmonary arterial endothelial cells were isolated from segments of calf pulmonary artery obtained from a local slaughterhouse, and cells between *passages 4* and *20* were grown to confluence (determined by phase-contrast microscopy) on gelatin-coated Biosilon microcarrier beads (mean diameter 230 μm; surface area 255 cm^2/g beads) in magnetic stirrer bottles (Techne, Burlington, NJ) containing RPMI 1640 medium supplemented with 20% fetal calf serum, 100 U/ml penicillin, 100 μg/ml streptomycin, and 30 mg/ml l-glutamine as previously described (31).

The hyperoxic exposure was accomplished as previously described by connecting a gas tank filled with 95% O_2-5% CO_2 to one of the side arms of the culture stirrer bottles by a length of tubing that was fitted through an opening in the back wall of the incubator (28). The other side arm was fitted with tubing that exited the incubator opening and was immersed in water to a depth of ~3 cm. The latter was to allow for visualization of gas flow through the bottle via bubble formation in the water. The gas flow rate was ~5 ml/min over a period of ~24–72 h, with the time interval between 48 and 54 h designated hereafter as hyperoxia exposed. The normoxic cells were exposed to the incubator gas mixture (95% air-5% CO_2). After 24 h of gassing, this procedure resulted in cell medium Po_2 of 550.9 ± 15.5 and 122.9 ± 1.1 mmHg (means ± SE), Pco_2 of 35.2 ± 0.2 and 34.8 ± 0.3 mmHg, and pH values of 7.24 ± 0.10 and 7.31 ± 0.10 for the hyperoxia-exposed and normoxic exposures, respectively (n = 4).

Protocols for measuring reduction of CoQ_1 and other electron acceptors (DQ and $TBOP^+$) by intact cells.

For each experimental sample, ~0.3-ml packed volume of cell-coated beads (160 cm^2 cell culture surface area/ml beads) was aliquoted into a 55 × 10 × 10-mm acrylic spectrophotometric cuvette (Sarstedt, Newton, NC). After the cell-coated beads had settled, they were washed three consecutive times by resuspension in 3 ml of room air-saturated Hanks' balanced salt solution (HBSS) containing 5.5 mM glucose and 10 mM HEPES (HBSS/HEPES), pH 7.4, and the beads were allowed to settle between each wash. The HBSS/HEPES was the experimental medium in all experiments that follow.

The washed cell-coated beads were resuspended in 3 ml of room air-saturated HBSS/HEPES at 37°C containing CoQ_1 (50 μM) and allowed to settle below the level of the spectrophotometer light path. The absorbance spectrum of the medium was measured between 250 and 350 nm by using a model DU 7400 spectrophotometer (Beckman Coulter). The capped cuvettes were placed on a Nutator mixer in a 37°C incubator, and periodically, the mixing was stopped and the cell-coated beads were allowed to settle for measurement of the medium absorbance spectrum. At the end of the incubation period, the medium was removed from the cells, and H_2O_2 (final concentration 0.1 mM) and peroxidase (final concentration 1.48 U/ml) were added to the cell-free medium to oxidize any CoQ_1H_2 to CoQ_1. The absorbance spectrum was measured again to determine the total concentration of CoQ_1 present, and the difference between the CoQ_1 concentration before and after the oxidation procedure was used to determine the CoQ_1H_2 concentration that was in the medium surrounding the cells at the end of the 30-min incubation period. The concentrations of CoQ_1 were calculated as the difference between the absorbance values at 281 and 294 nm to correct for crossover from CoQ_1H_2 absorbance, using the extinction coefficient 8.27 $mM^{-1}\cdot cm^{-1}$. The same protocol was used in an additional study with the cuvettes only, without cells present, to control for nonspecific association of CoQ_1 with the cuvettes.

CoQ_1-, DQ-, or $TBOP^+$-mediated reduction of the cell membrane-impermeant secondary electron acceptor ferricyanide was measured using protocols previously described for DQ and $TBOP^+$ (9, 28–31). After the cell-coated beads were washed free of culture medium as described above, 3 ml of HBSS/HEPES containing 600 μM ferricyanide in the absence or presence of CoQ_1 (1–50 μM), DQ (50 μM), or TBOP (0.2 mg/ml) were added to the cells. The cells were mixed with the medium as described above, and periodically the mixing was stopped and the absorbance of ferricyanide in the medium measured at 421 nm. The amount of the ferricyanide reduction product, ferrocyanide [$Fe(CN)_6^{4-}$] was calculated from the decrease in ferricyanide absorbance at each time point (extinction coefficient 1.0 $mM^{-1}\cdot cm^{-1}$). Additional experiments utilizing the ferricyanide protocol were performed in which the NQO1 inhibitors dicumarol (10 μM) or ES936 (0.5 μM) or the complex I inhibitor rotenone (1 μM) was added to the medium along with the ferricyanide and CoQ_1 or DQ.

CoQ_1-, DQ-, or $TBOP^+$-mediated ferricyanide reduction rates were determined from linear regression fits to the individual ferricyanide vs. time curves (9, 28–31). The background rates of cell-mediated ferricyanide reduction in the absence of CoQ_1, DQ, or TBOP were subtracted from the individual rates obtained in their presence and normalized to the cell protein, and then the data from the individual experiments were combined to obtain mean rates. The reduction rates for CoQ_1, DQ or $TBOP^+$ were calculated as one-half the zero-order ferricyanide reduction rates in the presence of the electron acceptors. The underlying assumptions are that CoQ_1 and DQ are freely permeable to intracellular sites of reduction and that CoQ_1H_2 and DQH_2 are freely permeable to intracellular sites of oxidation, whereas $TBOP^+$ is reduced at the cell surface via TPMET (9, 28). The assumption that both CoQ_1 and CoQ_1H_2 are freely cell membrane permeant is based on their high octanol:water partition coefficients [$\log_{10}$ octanol:water partition coefficient >3 for both redox forms (37)] and studies in the perfused rat lung (unpublished data) revealing a “flow-limited” behavior for CoQ_1H_2, consistent with freely permeating access to lung tissue from the vascular space. An additional assumption is that since ferricyanide reduction by CoQ_1H_2, DQH_2, and the reduced form of $TBOP^+$, TBOPH, is virtually instantaneous on the time course of the experiments, ferricyanide acts as an extracellular sink for the hydroquinones or TBOPH generated by the cells, thereby minimizing the contribution of cell-mediated oxidation of CoQ_1H_2, DQH_2, or TBOPH to the net effect of the cells on the compounds (9, 28–31).

HPLC measurements of CoQ_1 and CoQ_1H_2.

HPLC measurements of medium CoQ_1 and CoQ_1H_2 concentrations following 30-min incubations of the cells with CoQ_1 were carried out under the incubation conditions described above, using a previously described HPLC system (4, 30). CoQ_1 and CoQ_1H_2 were separated using a Supelcosil octadecylsilane LC-18-T (3-μm particle size, 150 × 4.6 mm) column eluted with methanol-H_2O-trifluoroacetic acid (70:30:0.1 vol/vol/vol) containing 50 mM acetic acid. The mobile phase was continuously sparged with N_2 for at least 15 h before and throughout the course of the HPLC studies. The CoQ_1 in the column eluate was measured by absorbance at 270 nm. CoQ_1H_2 was detected electrochemically, with the potentials at the first and second analytical electrodes set at −250 and +500 mV, respectively. The first electrode served as a screen electrode to prevent interference from compounds that might coelute with CoQ_1H_2 but have a lower oxidation potential. The CoQ_1H_2 was oxidized at the second electrode. The elution times were 7.86 ± 0.04 min for CoQ_1 and 5.21 ± 0.02 min for CoQ_1H_2 for 12 injections each.

The concentration of CoQ_1 was determined by peak area quantification against a standard curve. To account for any CoQ_1 present in the CoQ_1H_2 standards (typically ∼5–10% of the total), the CoQ_1H_2 standard curve was calibrated by determining the CoQ_1 concentration in each standard, as measured by HPLC, before and after the addition of H_2O_2 (final concentration 0.1 mM) and peroxidase (final concentration 1.48 U/ml), to fully oxidize the sample. The standard curves were linear over the CoQ_1 and CoQ_1H_2 concentration ranges studied.

Protocols for measuring CoQ_1H_2 oxidation by intact cells.

Cell-coated beads in spectrophotometric cuvettes were washed free of culture medium and resuspended in 3 ml of room air-saturated HBSS/HEPES containing CoQ_1H_2 (50 μM) without and with the addition of the mitochondrial electron transport complex III inhibitors myxothiazol (2 μM) and antimcycin A (2 μM). The cell-coated beads were allowed to settle below the level of the spectrophotometer light path, and the absorbance spectrum of the medium was measured between 250 and 350 nm. The capped cuvettes were placed on a Nutator mixer in a 37°C incubator, and periodically, the mixing was stopped and the cell-coated beads were allowed to settle for measurement of the medium absorbance spectrum. CoQ_1 concentrations were determined as described above. CoQ_1H_2 autooxidation under the study conditions was evaluated using the same protocol, except that there were no cells present.

Complex I and complex IV (cytochrome oxidase) activity assays.

A ~3-ml packed volume of cell-coated beads was washed by resuspension and settling in 5 ml of phosphate-buffered saline (PBS), followed by 5 ml of Dulbecco's phosphate-buffered saline (D-PBS) containing 0.5 mM EDTA. The cells were detached from the microcarrier beads by trypsinization. The mitochondria-enriched fractions were prepared from the cells using the mitochondria isolation kit for cultured cells (catalog no. 89874; Pierce, Rockford IL) essentially as described by the manufacturer, following option B, and using a Wheaton Potter-Elvehjem tissue grinder to disrupt the cells (60 strokes). For 21 preparations from normoxic and hyperoxia-exposed cells, the mitochondria-enriched fraction protein collected was 0.42 ± 0.06 mg. The mitochondrial preparations were frozen at −80°C. Assay of complex I was as described previously (27), wherein ~0.2 mg of the thawed mitochondria-enriched fraction was mixed in a solution containing 50 mM KCl, 1 mM EDTA, 10 mM Tris·HCl, 1 mM cyanide, and 10 μM antimycin (pH 7.4) in the presence or absence of rotenone (20 μM) or rolliniastatin-2 (3 μM), the latter of which was the kind gift of Dr. Giorgio Lenaz (Dipartimento di Biochimica, Universitá de Bologna, Bologna, Italy). Reactions were carried out at room temperature and initiated by addition of NADH (final concentration 100 μM) and CoQ_1 (final concentration 100 μM). The decrease in absorbance at 340 nm was used to calculate the NADH oxidation rate using an extinction coefficient of 6.22 $mM^{-1}{\cdot}cm^{-1}$. The rates were normalized to milligrams of mitochondria-enriched fraction protein, and the complex I activity was calculated by subtracting the NADH oxidation rates measured in the absence and presence of the complex I inhibitors.

Complex IV activity was determined as described previously (43). Ferrocytochrome *c* was mixed with ~0.04 mg of thawed mitochondria-enriched fraction protein in phosphate buffer containing 0.1% Triton X-100 (pH 6.2) at room temperature, and the decrease in absorbance was measured at 550 nm. The ferrocytochrome *c* oxidation rate was determined using an extinction coefficient of 19.1 $mM^{-1}{\cdot}cm^{-1}$ and normalized to milligrams of mitochondria-enriched fraction protein.

Cellular oxygen consumption.

Cellular oxygen consumption was measured using a Yellow Springs Instruments model 5300 biological oxygen monitor (YSI, Yellow Springs, OH) as previously described (28, 30). Cell-coated beads were added to 3 ml of air-saturated HBSS/HEPES (initial O_2 concentration 224 μM) in sealed magnetically stirred chambers at 37°C. Data collection rate was every 2 s (DATAQ Instruments, Akron, OH). The rate of oxygen consumption was calculated as the decrease in buffer O_2 concentration over a period of ~15 min following the addition of cells to the chamber and over the same time period following additions of rotenone (5 μM) or 2,4-dinitrophenol (DNP; 50 μM) to the cell suspensions in the oximeter chambers.

Cell viability and protein content.

At the end of the experiments, for each cell sample, the medium was removed from the cells and the cells were lysed by sonication as previously described (9, 28–31). Lactate dehydrogenase (LDH) activity in the medium and cells lysate was determined as described, and the cell lysate protein content was measured using the Bio-Rad protein assay (9, 28–31).

Statistical analysis.

Mean values for normoxic and hyperoxia-exposed cell treatments were compared using the Student's *t*-test or ANOVA followed by Tukey's post hoc test. Differences were considered significant at the $P < 0.05$ level.

RESULTS

Figure 1*A* shows spectrophotometric measurements of CoQ_1 concentrations in the medium of normoxic and hyperoxia-exposed cells incubated with 50 μM CoQ_1 for 30 min. The medium CoQ_1 concentrations decreased over time, reaching a lower level for the normoxic than hyperoxia-exposed cells by 5 min and remaining lower for the normoxic cells throughout the incubation period. The decreases were in part attributable to cell-dependent reduction of CoQ_1 to the hydroquinone (CoQ_1H_2), wherein the normoxic cells generated ~3.4 times more extracellular CoQ_1H_2 than the hyperoxia-exposed cells by the end of the 30-min incubation period (Fig. 1*B*).

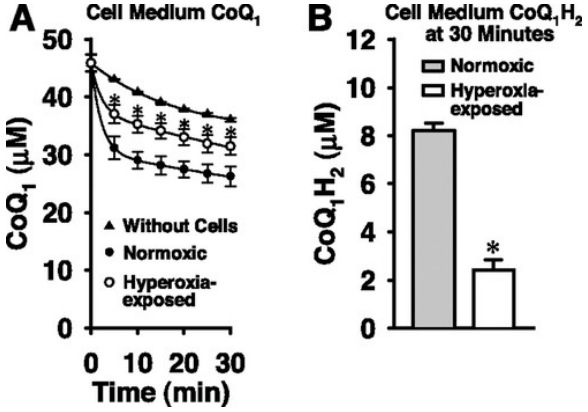

Fig. 1. Spectrophotometric measurements of coenzyme Q_1 (CoQ_1) and CoQ_1 hydroquinone (CoQ_1H_2) in medium surrounding normoxic and hyperoxia-exposed pulmonary arterial endothelial cells incubated with CoQ_1. *A*: CoQ_1 concentrations in the medium of normoxic and hyperoxia-exposed cell-coated microcarrier beads after addition of 50 μM CoQ_1. Also shown are the CoQ_1 concentrations in the medium over the same experimental time course in the absence of cells. Data are means ± SE for $n = 5$ each for the normoxic and hyperoxia-exposed cells and $n = 6$ for the medium without cells. Cell proteins (means ± SE) were 1.51 ± 0.06 and 1.60 ± 0.08 mg for the normoxic and hyperoxia-exposed cells, respectively. *$P < 0.05$, significantly different from the CoQ_1 concentration in the normoxic cell medium at the corresponding time point. *B*: CoQ_1H_2 concentrations in the medium at the end of the 30-min incubation period in *A*. *$P < 0.05$, significantly different from the CoQ_1H_2 concentration in the normoxic cell medium.

As shown in Fig. 1, the CoQ_1 concentration in the medium also decreased over the experimental time course even in the absence of cells, wherein 72.1 ± 0.5% of the CoQ_1 originally added to the medium was remaining at the end of the 30-min incubation period. This was analogous to observations with DQ, wherein the loss was attributed to binding to the experimental plasticware (30). Of the CoQ_1 originally added to the normoxic and hyperoxia-exposed cell medium, 68.9 ± 3.0 and 67.8 ± 3.4%, respectively, was recovered in the extracellular medium as CoQ_1 + CoQ_1H_2 at the end of the 30-min incubation period. The percent recoveries in the absence and presence of cells were not significantly different (ANOVA, $P = 0.44$), suggesting that the incomplete recovery in the medium surrounding the cells was attributable predominately to CoQ_1 binding to the plasticware.

Figure 2 shows HPLC measurements of CoQ_1 and CoQ_1H_2 in the medium of normoxic and hyperoxia-exposed cells after 15 min of incubation with 50 μM CoQ_1 under the same conditions as in Fig. 1. About 3.5 times more CoQ_1H_2 was detected in the medium surrounding the normoxic than the hyperoxia-exposed cells, which was consistent with the spectrophotometric measurements in Fig. 1*B*.

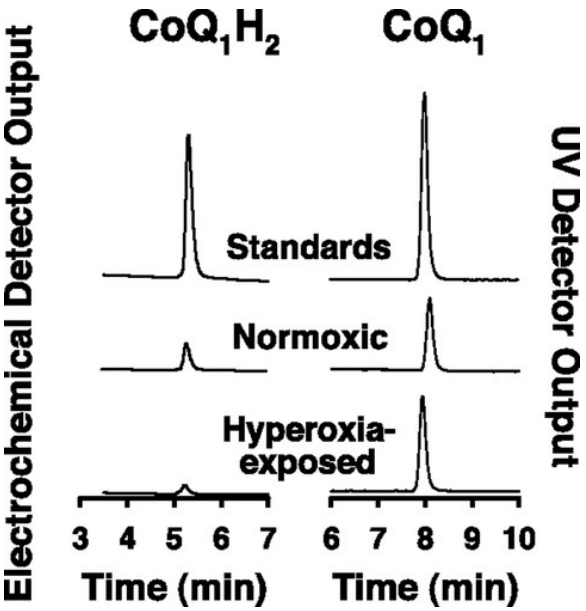

Fig. 2.HPLC measurements of CoQ_1H_2 and CoQ_1 in medium surrounding normoxic and hyperoxia-exposed pulmonary arterial endothelial cells incubated with CoQ_1 (50 μM). CoQ_1H_2 and CoQ_1 standards were 39.4 and 50.2 μM, respectively. After 15 min of incubation under the same conditions as described in Fig. 1, the cell medium concentrations of CoQ_1H_2 and CoQ_1 were 7.3 and 19.5 μM, respectively, for the normoxic cells and 2.1 and 25.6 μM, respectively, for the hyperoxia-exposed cells. The 2 detector signals were scaled such that the area of the CoQ_1 peak = area of CoQ_1H_2 peak at equimolar concentrations. Cell proteins were 0.8 and 0.7 mg for the normoxic and hyperoxia-exposed cells, respectively.

Figure 3 shows spectrophotometric measurements of CoQ_1 concentrations in the medium of normoxic and hyperoxia-exposed cells incubated with 50 μM CoQ_1H_2 for 30 min. The medium CoQ_1 concentrations increased at a similar rate for the normoxic and hyperoxia-exposed cells for the first ~5 min, after which time they tended to level off, albeit at a lower concentration for the normoxic than hyperoxia-exposed cells. There was no significant difference between the amount of total CoQ_1 + CoQ_1H_2 recovered in the medium at the end of the 30-min incubation period for the normoxic and hyperoxia-exposed cells ($P > 0.05$). The generation of CoQ_1 from CoQ_1H_2 was primarily cell dependent, since the CoQ_1H_2 autooxidation rate in the absence of cells was relatively very slow (Fig. 3). The mitochondrial electron transport complex III inhibitors myxothiazol (2 μM) and antimycin A (2 μM) largely blocked the appearance of CoQ_1 when normoxic or hyperoxia-exposed cells were incubated with CoQ_1H_2, suggesting complex III as the dominant site of CoQ_1H_2 oxidation.

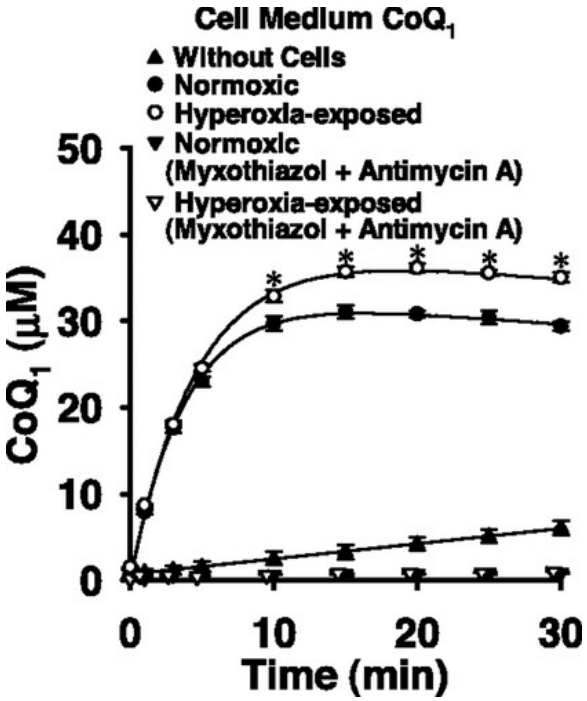

Fig. 3. Spectrophotometric measurements of CoQ_1 in medium surrounding normoxic and hyperoxia-exposed pulmonary arterial endothelial cells incubated with CoQ_1H_2. CoQ_1 concentrations were measured in the medium after the addition of 50 μM CoQ_1H_2 to the normoxic and hyperoxia-exposed cell-coated microcarrier beads without and with the complex III inhibitors myxothiazol (2 μM) and antimycin A (2 μM). Also shown are the CoQ_1 concentrations in the medium in the absence of cells. Data are means ± SE for n = 3 each. Cell proteins (means ± SE) were 0.67 ± 0.03, 0.73 ± 0.02, 0.69 ± 0.02, and 0.71 ± 0.01 mg for the normoxic, hyperoxia-exposed, normoxic + myxothiazol + antimycin A, and hyperoxia-exposed + myxothiazol + antimycin A cells, respectively. *P < 0.05, significantly different from the CoQ_1 concentration in the normoxic cell medium at the corresponding time point.

Together, the data in Figs. 1–3 suggested that the impact of the cells on CoQ_1 and CoQ_1H_2 was a result of both CoQ_1 reduction and CoQ_1H_2 oxidation reactions. The net effect was that regardless of whether CoQ_1 or CoQ_1H_2 was initially added, the CoQ_1 concentration approached a quasi-steady state that was higher for hyperoxia-exposed than normoxic cells. Since the small difference between the quasi-steady-state CoQ_1 concentrations attained for the normoxic and hyperoxia-exposed cells [~5 μM CoQ_1 (Fig. 1 or 3)] could potentially mask a large difference in CoQ_1 reduction and/or CoQ_1 oxidation rate(s), a means to separate the two rates was required to interpret the data. The secondary cell membrane impermeant redox indicator ferricyanide has proved useful for unmasking the quinone reduction component from the net effect of the cells on the quinones by minimizing the contribution of cell-mediated hydroquinone oxidation. It does so by virtually instantaneously oxidizing cell-generated hydroquinone, acting as a hydroquinone sink. The ferricyanide reduction rate thereby provides an estimation of the rate of hydroquinone appearance, or quinone reduction (see materials and methods and Refs. 9, 28–31).

Figure 4*A* shows that ferricyanide reduction by normoxic or hyperoxia-exposed cells proceeded relatively slowly in the absence of CoQ_1. However, when 50 μM CoQ_1 was present along with ferricyanide, the amount of ferricyanide in the medium decreased over time. This was indicative of ferricyanide reduction to ferrocyanide by the cell-generated CoQ_1H_2, wherein the net reaction followed zero-order kinetics (Fig. 4*A*). The rate of CoQ_1 reduction to CoQ_1H_2, calculated as one-half the CoQ_1-mediated ferricyanide reduction rate, was about twice as fast for the normoxic as the hyperoxia-exposed cells (Fig. 4*B*). When studied over the

CoQ_1 concentration range of 1–50 μM, the normoxic cell-mediated CoQ_1 reduction rates were faster than the hyperoxia-exposed cells at concentrations >10 μM (Fig. 5). The decrease in CoQ_1 reduction capacity in the hyperoxia-exposed cells was not associated with a detectable decrease in cell protein, cell viability measured as %LDH release, or total LDH activity compared with normoxic cells (Table 1). Furthermore, the effect on CoQ_1 was apparently not indicative of a general decline in cell redox function, since the DQ reduction rate as a measure of NQO1 activity was higher for the hyperoxia-exposed than normoxic cells (Fig. 6, *A* and *B*), consistent with our previous observations (28, 30), whereas TPMET-mediated $TBOP^+$ reduction rates were comparable for the normoxic and hyperoxia-exposed cells (Fig. 6, *C* and *D*).

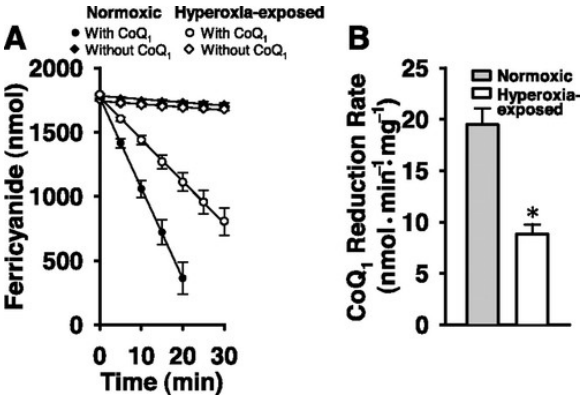

Fig. 4.CoQ_1 reduction by normoxic and hyperoxia-exposed cells measured using ferricyanide. *A*: decrease in total ferricyanide in the medium after addition of either ferricyanide (600 μM) alone or ferricyanide (600 μM) + CoQ_1 (50 μM) to the extracellular medium. Data are means ± SE for $n = 17$ each for the normoxic and hyperoxia-exposed cell studies with CoQ_1 and $n = 4$ each without CoQ_1. The lines are linear regression fits to the data. Cell proteins (means ± SE) for the normoxic and hyperoxia-exposed cell studies with CoQ_1 were 1.72 ± 0.31 and 1.78 ± 0.3 mg, respectively, and 1.84 ± 0.13 and 1.80 ± 0.14 mg, respectively, without CoQ_1. *B*: CoQ_1 reduction rates were obtained from independent linear regression model fits to 17 normoxic and 17 hyperoxia-exposed cell data sets, with the mean ferricyanide-only rate ($n = 4$) subtracted from each, with each of the resulting rates normalized to cell protein. Data are means ± SE of the CoQ_1 reduction rates, which were calculated as one-half the zero-order CoQ_1-mediated ferricyanide reduction rates, under assumptions stated in materials and methods and in Refs. 38 and 40. *$P < 0.05$, significantly different from normoxic cells.

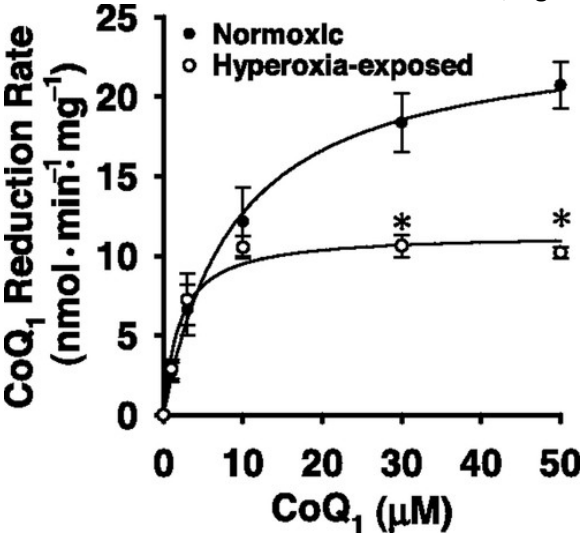

Fig. 5. Effect of CoQ_1 concentration on CoQ_1 reduction rates in normoxic and hyperoxia-exposed cells. The reduction rates of CoQ_1 (1–50 μM) measured using 600 μM ferricyanide and normalized to cell protein. Data represent the CoQ_1 reduction rates, calculated as described in Fig. 4 from the mean ± SE of $n = 4$ each normoxic and hyperoxia-exposed cell CoQ_1 concentration response curves, for a total of 23 data points for each cell type. The lines represent Michaelis-Menten model fits to the data. The estimated values of V_{max} from the model fit to

the data were 24.1 and 11.4 nmol·min^{-1}·mg cell protein^{-1}, and the estimated K_m values were 8.9 and 2.0 μM for the normoxic and hyperoxia-exposed cells, respectively. Cell proteins (means ± SE) for the normoxic and hyperoxia-exposed cell studies were 1.78 ± 0.13 and 1.88 ± 0.14 mg, respectively. *P < 0.05, significantly different from normoxic cells at the same CoQ_1 concentration.

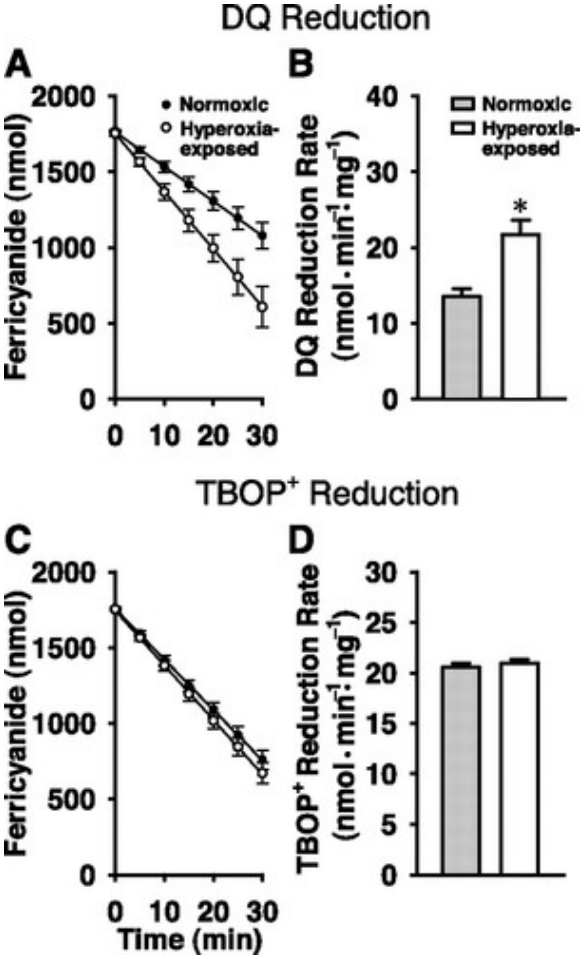

Fig. 6. Duroquinone (DQ) and toluidine blue O polyacrylamide ($TBOP^+$) reduction by normoxic and hyperoxia-exposed cells measured using ferricyanide. The total medium ferricyanide following addition of 600 μM ferricyanide and 50 μM DQ (*A*) or 600 μM ferricyanide and 0.2 mg/ml TBOP (*C*) to the normoxic and hyperoxia-exposed cells. Data are means ± SE from *n* = 4 each of the normoxic and hyperoxia-exposed cell studies. The lines represent linear regression fits to the data. Cell proteins (means ± SE) were 1.70 ± 0.2 and 1.75 ± 0.15 mg (*A*) and 1.63 ± 0.13 and 1.73 ± 0.14 mg (*C*) for the normoxic and hyperoxia-exposed cells, respectively. *B* and *D*: DQ and $TBOP^+$ reduction rates (means ± SE), respectively, obtained from the data in *A* and *C*, as described in the legend to Fig. 4 for CoQ_1. *P < 0.05, significantly different from normoxic cells.

Table 1. Normoxic and hyperoxia-exposed cell protein, cell viability (%LDH release), and total cell LDH activity

	Cell Protein, g/cm^2	Cell Viability, %LDH release	Total Cell LDH Activity, units/ g protein	Total Cell LDH Activity, units/cm^2
Normoxic	30.7±1.1	2.6±0.2	3.0±0.1	90.3±3.4
Hyperoxia-exposed	31.4±1.1	2.8±0.2	3.1±0.1	95.5±3.7

Data are means ± SE (*n* = 77 for each measurement) of normoxic and hyperoxia-exposed (95% O_2, 48 h) cell protein normalized to cell culture surface area, cell viability measured as the percentage of total cell lactate dehydrogenase (LDH) released from the cells into the medium and total cell LDH activity normalized to cell protein or cell culture surface area. No significant differences between groups by *t*-test (*P* > 0.05).

Quinone reductase inhibitors were used to evaluate the mechanism(s) of pulmonary endothelial cell-mediated CoQ_1 reduction. There was no significant effect of the competitive and mechanism-based NQO1 inhibitors dicumarol or ES936, respectively, on CoQ_1 reduction rates for the normoxic cells (Fig. 7, *A* and *C*) and little, if any, for the hyperoxia-exposed cells (Fig. 7, *B* and *D*). Yet, the same concentration of dicumarol nearly completely blocked DQ reduction in both normoxic and hyperoxia-exposed cells, consistent with previous observations (Fig. 7, *E* and *F*) (28, 30). On the other hand, the mitochondrial electron transport complex I inhibitor rotenone decreased the CoQ_1 reduction rate in both normoxic and hyperoxia-exposed cells (Fig. 8). Rotenone decreased the normoxic cell mediated reduction rate from 22.3 to 3.2 $nmol \cdot min^{-1} \cdot mg$ cell $protein^{-1}$ (Fig. 8*A*) and the hyperoxia-exposed cell rate from 10.1 to 5.7 $nmol \cdot min^{-1} \cdot mg$ cell $protein^{-1}$ (Fig. 8*B*).

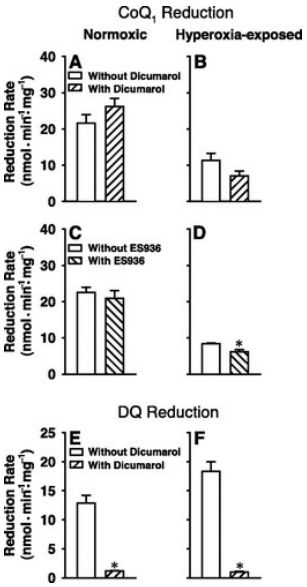

Fig. 7. Effect of NAD(P)H:quinone oxidoreductase 1 (NQO1) inhibition on CoQ_1 and DQ reduction rates in normoxic and hyperoxia-exposed cells. *A*–*D*: CoQ_1 reduction by normoxic (*A*) and hyperoxia-exposed cells (*B*) without and with dicumarol (10 μM) and by normoxic (*C*) and hyperoxia-exposed cells (*D*) without and with ES936 (0.5 μM). *E* and *F*: DQ reduction by normoxic (*E*) and hyperoxia-exposed cells (*F*) without and with dicumarol (10 μM). Reduction rates were determined using 600 μM ferricyanide and 50 μM CoQ_1 or DQ and normalized to cell protein as described for Fig. 4. Cell proteins (means ± SE), without and with inhibitors, respectively, were 1.98 ± 0.4 and 1.81 ± 0.22 mg (*A*), 1.75 ± 0.25 and 1.78 ± 0.26 mg (*B*), 2.06 ± 0.27 and 2.22 ± 0.32 mg (*C*), 1.95 ± 0.11 and 2.06 ± 0.23 mg (*D*), 2.21 ± 0.34 and 2.11 ± 0.33 mg (*E*), and 2.48 ± 0.27 and 2.27 ± 0.30 mg (*F*). The number of experiments was $n = 6$ each in *A* and *B*, $n = 4$ each in *C* and *D*, and $n = 3$ each in *E* and *F*. *$P < 0.05$, significantly different from values without dicumarol or ES936.

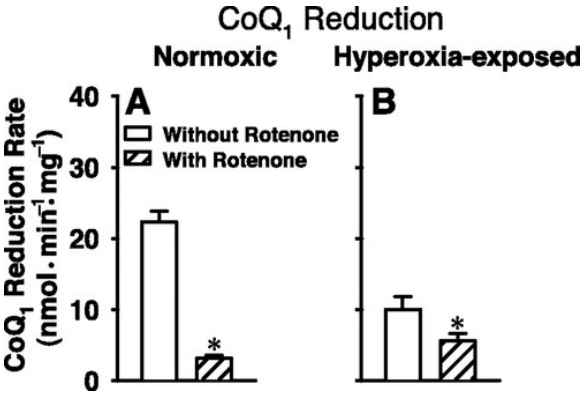

Fig. 8. Effect of complex I inhibition on CoQ_1 reduction rates in normoxic and hyperoxia-exposed cells. Reduction rate of 50 µM CoQ_1 normalized to cell protein by normoxic (*A*) and hyperoxia-exposed cells (*B*) without and with rotenone (1 µM). Reduction rates were determined using 50 µM CoQ_1 and 600 µM ferricyanide as described for Fig. 4. Cell proteins (means ± SE) without and with rotenone, respectively, were 1.77 ± 0.2 and 1.59 ± 0.17 mg for normoxic cells and 1.83 ± 0.28 and 1.77 ± 0.33 mg for hyperoxia-exposed cells. The number of experiments was $n = 6$ for each condition. *$P < 0.05$, significantly different from values without rotenone.

The effect of rotenone implied a role of complex I in CoQ_1 reduction, with the decrease in rotenone-sensitive reduction capacity in the hyperoxia-exposed cells suggesting a decrease in complex I activity. That the hyperoxic response included altered mitochondrial quinone oxidoreductase activity was further suggested by the observation that basal oxygen consumption was lower in the hyperoxia-exposed cells (Fig. 9, *A* and *B*). As shown in the example in Fig. 9*A*, rotenone nearly completely blocked oxygen consumption in both normoxic and hyperoxia-exposed cells, whereas the pharmacological uncoupler DNP increased the oxygen consumption rate in normoxic but not hyperoxia-exposed cells. The rotenone-sensitive oxygen consumption rates in the absence and presence of DNP for the entire data set are summarized in Fig. 9*B*.

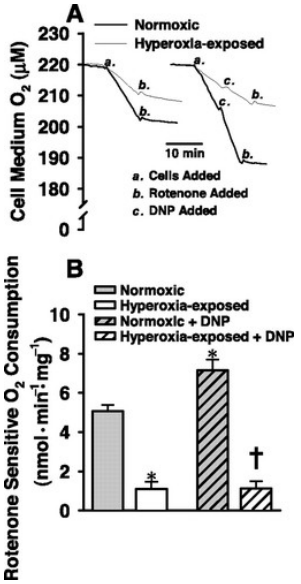

Fig. 9. Oxygen consumption by intact normoxic and hyperoxia-exposed cells. *A*: a representative tracing of oxygen consumption by normoxic and hyperoxia-exposed cells. At *left*, measurement of background oxygen consumption (in the absence of cells) was followed by addition of the cells to the oximeter chambers at *a* and rotenone at *b*. Cell proteins were 1.15 and 1.71 mg for the normoxic and hyperoxia-exposed cells, respectively. At *right*, measurement of the background oxygen consumption in the absence of cells was followed by addition of cells at *a*, 2,4-dinitrophenol (DNP; 50 µM) at *c*, and rotenone (5 µM) at *b*. Cell proteins were 1.23 and 1.60 mg

for the normoxic and hyperoxia-exposed cells, respectively. *B*: rotenone-sensitive oxygen consumption rates (means ± SE) for normoxic (*n* = 12), hyperoxia-exposed (*n* = 6), normoxic + DNP (*n* = 9) and hyperoxia-exposed + DNP cells (*n* = 6). Cell proteins (means ± SE) were 1.34 ± 0.09, 1.78 ± 0.05, 1.20 ± 0.08, and 1.70 ± 0.02 mg for the normoxic, hyperoxia-exposed, normoxic +DNP and hyperoxia-exposed + DNP cells, respectively. **P* < 0.05, significantly different from normoxic cells. †*P* < 0.05, hyperoxia-exposed + DNP vs. normoxic cells + DNP (2-way ANOVA and post hoc Tukey's test).

Consistent with the CoQ_1 reduction and oxygen consumption studies, complex I activity in mitochondria-enriched fractions from hyperoxia-exposed cells was lower than that measured in fractions from normoxic cells (Fig. 10*A*). However, there was no detectable difference between the normoxic and hyperoxia-exposed cell complex IV activities in the mitochondria-enriched fractions (Fig. 10*B*).

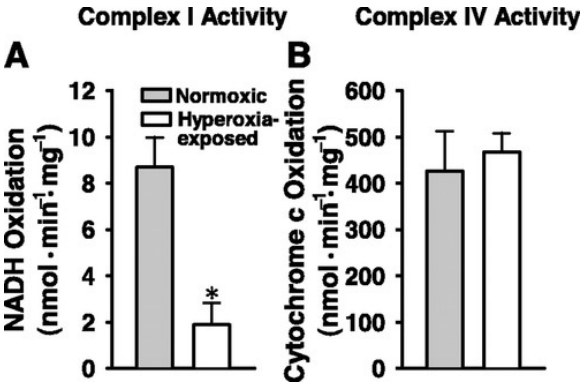

Fig. 10. Complex I and IV activity in mitochondria-enriched fractions from normoxic and hyperoxia-exposed cells. *A*: complex I activities for normoxic (*n* = 8) and hyperoxia-exposed (*n* = 9) cells. *B*: complex IV activities for normoxic and hyperoxia-exposed cells (*n* = 4 each). **P* < 0.05, significantly different from normoxic cells.

Whereas the studies in Figs. 1–10 were focused on 48 h of hyperoxic exposure, the data in Fig. 11 show that the effect of hyperoxia on CoQ_1 reduction was evident by 24 h of exposure, with no additional effects up to 72 h (Fig. 11*A*). In contrast to the time course and direction of the hyperoxic effect on CoQ_1 reduction, the hyperoxia-induced increase in DQ reduction rate was not observed until 48 h of exposure, with a further increase seen at 72 h (Fig. 11, *A* and *B*). There was no detectable effect of hyperoxia on $TBOP^+$ reduction via TPMET at any of the hyperoxic exposure times studied (Fig. 11*C*).

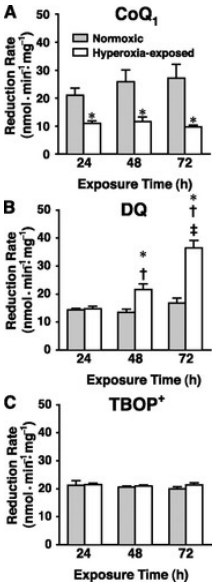

Fig. 11. Effect of duration of hyperoxic exposure on CoQ_1, DQ, and $TBOP^+$ reduction rates. CoQ_1 (*A*), DQ (*B*), and $TBOP^+$ (*C*) reduction rates normalized to cell protein measured at 24, 48, and 72 h following initiation of hyperoxic exposure. Reduction rates were measured using 600 μM ferricyanide and 50 μM CoQ_1, 50 μM DQ, or 0.2 mg/ml TBOP and calculated as described in Fig. 4. Cell proteins (means ± SE) for the normoxic and hyperoxia-exposed cells were, respectively, 1.45 ± 0.05 and 1.50 ± 0.07 mg at 24 h, 1.67 ± 0.08 and 1.68 ± 0.06 mg at 48 h, and 1.62 ± 0.05 and 1.67 ± 0.06 mg at 72 h; *n* = 4 experiments for each condition. Lactate dehydrogenase (LDH) release (means ± SE) for the normoxic and hyperoxia-exposed cells were, respectively, 2.0 ± 0.3 and 1.6 ± 0.2% at 24 h, 1.5 ± 0.2 and 1.8 ± 0.2% at 48 h, and 1.4 ± 0.2 and 1.7 ± 0.2% at 72 h. There were no significant differences between the normoxic and hyperoxia-exposed cell %LDH release at any given time point ($P > 0.05$). *$P < 0.05$, significantly different from normoxic cells at the corresponding time point. †$P < 0.05$, significantly different from hyperoxia-exposed cells at 24 h. ‡$P < 0.05$, significantly different from hyperoxia-exposed cells at 48 h.

DISCUSSION

The results of the present study demonstrate that intact normoxic and hyperoxia-exposed bovine pulmonary arterial endothelial cells reduce CoQ_1, observed either as the appearance of CoQ_1H_2 in the extracellular medium (Figs. 1*B* and 2) or as CoQ_1-mediated reduction of the cell membrane-impermeant secondary electron acceptor ferricyanide (Fig. 4). The apparent maximum CoQ_1 reduction rate (V_{max}) calculated from the Michaelis-Menten model fit to the CoQ_1-mediated ferricyanide reduction rates over a range of CoQ_1 concentrations was approximately twofold higher for the normoxic compared with hyperoxia-exposed cells (24.1 and 11.4 $nmol \cdot min^{-1} \cdot mg^{-1}$ cell protein, respectively) (Fig. 5). This difference apparently contributed to the observation that the extracellular $[CoQ_1H_2]/[CoQ_1]$ ratio in the extracellular medium of normoxic cells was approximately fourfold higher than that of the hyperoxia-exposed cells following incubation with 50 μM CoQ_1.

The data also revealed a complex III-mediated CoQ_1H_2 oxidation process that contributed to net effect of the cells on the extracellular CoQ_1 redox status. This was manifested by the appearance of CoQ_1 in the medium of cells incubated with CoQ_1H_2, wherein the CoQ_1 appearance rate could not be accounted for by CoQ_1H_2 autooxidation (Fig. 3). In addition, cell-mediated CoQ_1H_2 oxidation was blocked by the complex III inhibitors myxothiazol and antimycin A (Fig. 3). This was not unexpected, since complex III-mediated oxidation of CoQ_1H_2 was the proposed mechanism for CoQ_1-mediated restoration of electron transport in hepatocytes with complex I dysfunction (12). Studies were not carried out to evaluate the impact of hyperoxic exposure on CoQ_1H_2 oxidation kinetics, which would require additional studies of CoQ_1H_2 oxidation in the presence of inhibitors of CoQ_1 reduction. Thus the question remains whether a difference between normoxic and hyperoxia-exposed cell oxidation kinetics contributed to the differences between the net effects on CoQ_1 redox status. However, previous studies demonstrated that DQH_2 was also oxidized via complex III in the pulmonary endothelial cells and that oxidation kinetics in normoxic and hyperoxia-exposed cells were reasonably comparable in the presence of dicumarol, the latter of which was included to suppress NQO1-mediated DQ reduction for measurement of oxidation rates (28, 30). The study was interpreted to indicate that complex III activity was not compromised in hyperoxia-exposed cells, which, if true, would imply that that the differences between the impact of normoxic and hyperoxic-exposed cells on CoQ_1 redox status would be predominately a reflection of the differences in CoQ_1 reduction rates.

Evidence for a role of complex I in intact cell-mediated CoQ_1 reduction was revealed by the observation that rotenone inhibited the CoQ_1 (50 μM) reduction rates by ~85 and ~44% for the normoxic and hyperoxia-exposed cells, respectively (Fig. 8). The decrease in complex I activity in the mitochondria-enriched fractions of hyperoxia-exposed cells was consistent with the decreases in both total and rotenone-sensitive CoQ_1 reduction capacity in the intact hyperoxia-exposed cells (21). Although to our knowledge an effect of hyperoxia to depress complex I

activity has not been observed previously in pulmonary endothelial cells, it has been reported for Chinese hamster ovary (CHO) cells following a similar hyperoxic exposure protocol to that used in the present study (40). Depression of complex I activity has also been observed in other cell types and tissues in response to pro-oxidant stimuli, including doxorubicin-treated endothelial cells (25). A recent study suggestive of mitochondrial dysfunction in pediatric pulmonary hypertension reported that among the respiratory complexes, complex I was the most severely affected in the two patients studied (6).

To evaluate the utility of CoQ_1 as a quantitative probe of changes in complex I activity in intact cells, we compared the impact of hyperoxia on intact cell CoQ_1 reduction capacity, mitochondrial fraction complex I activity, and intact cell oxygen consumption. First, the fractional decrease in intact cell rotenone-sensitive CoQ_1 reduction rate (77% lower than normoxic cells, Fig. 8) and complex I activity in mitochondrial fractions (78% lower than normoxic cells, Fig. 10) was nearly the same. This suggested that the CoQ_1 reduction rate in the intact cells reflected the rate of electron flow through complex I. To obtain an independent estimate of the maximum rate of electron flow through complex I in the intact cell, we measured cell oxygen consumption in the presence of a mitochondrial uncoupler in the absence and presence of the complex I inhibitor rotenone (Fig. 9, *A* and *B*). Considering that reduction of CoQ_1 to CoQ_1H_2 via complex I requires 2 moles of electrons per mole of CoQ_1 reduced, whereas O_2 reduction via the electron transport chain utilizes 4 moles of electrons per mole O_2, there was a difference of 30 nmol·min^{-1}·mg cell protein^{-1} between normoxic and hyperoxia-exposed cells with respect to the rate of utilization of reducing equivalents for rotenone-sensitive CoQ_1 reduction and a difference of 24 nmol·min^{-1}·mg cell protein^{-1} for uncoupled, rotenone-sensitive O_2 reduction. These values are reasonably close, supporting the concept that intact cell CoQ_1 reduction rates, measured in the extracellular medium under certain defined experimental conditions (e.g., saturating CoQ_1 concentrations), can provide a reasonable approximation of the magnitude of changes in mitochondrial complex I activity in response to oxidative stress.

The intact cell complex I measurement using CoQ_1 may be distinguished from measurements in isolated mitochondria or submitochondrial particles in that it reflects not only the intrinsic activity of the complex but also other factors contributing to its activity under a given set of physiological or pathophysiological conditions. These may include a restriction in the availability of reducing equivalents produced via Krebs cycle enzymes, for example, via aconitase inactivation observed in hyperoxic exposure of lung and lung A549 cells (20). In the present study, the relationship between the effects of hyperoxia on complex I activity in the mitochondrial fractions (78% lower than normoxic cells) and on coupled rotenone-sensitive oxygen consumption (78% lower than normoxic cells) was reasonably consistent with that observed in a model of rotenone-induced complex I deficiency in human osteosarcoma-derived cells (7). In that study, ~80% inhibition of complex I activity was associated with ~60% decrease in total cellular oxygen consumption, wherein the latter decrease might have been expected to be even larger if the rotenone-sensitive fraction were considered. The implication is that for the hyperoxia-exposed cells, a defect in complex I provided a sufficient explanation for the depression in oxygen consumption. In this regard, it is the combined information contained in measurements of oxygen consumption, isolated mitochondrial complex I activity, and intact cell CoQ_1 reduction capacity that can provide insight into the role of complex I in mitochondrial dysfunction.

There were several indications that the effect of hyperoxia on complex I activity was not due to nonspecific depression of cell metabolism or redox function. First, there was no detectable difference between the cytochrome oxidase activities measured in the normoxic and hyperoxia-exposed cell mitochondrial fractions (Fig. 10*B*). The relative insensitivity of cytochrome oxidase activity compared with complex I activity in the hyperoxia-exposed cells was consistent with observations in bovine heart submitochondrial particles exposed to various reactive oxygen species (ROS) (45). The observations that the cell protein and viability (%LDH release) were equivalent for the normoxic and hyperoxia-exposed cells, as were the total LDH activities, wherein LDH

represents another cell redox enzyme, further suggested that the effect of hyperoxia was not as a widespread nonspecific toxicant. This concept is consistent with the fact that the DQ reduction capacity was actually higher in the hyperoxia-exposed than normoxic cells, as previously observed (28), whereas TPMET activity was unaffected.

The basis for the selectivity of CoQ_1, DQ and $TBOP^+$ for reduction via complex I, NQO1, and the TPMET system utilizing thiazine acceptors, respectively, is presumably their differing physical and/or chemical properties. TBOP is so large that it is excluded from the cell and is thereby reduced predominately at the cell surface (9). That CoQ_1 acted as a complex I substrate in the intact cells might have been anticipated from its utility as an amphipathic CoQ_{10} homolog in studies of complex I in mitochondria and submitochondrial fractions (16, 18, 33). CoQ_1 is reduced more rapidly than DQ via the NADH dehydrogenase activity of complex I in isolated mitochondria and displays a higher degree of rotenone sensitivity, whereas DQ has been considered a relatively "poor" acceptor for this enzyme (16, 18). The activity of CoQ_1 compared with DQ as a complex I substrate is not on the basis of solubility characteristics, which are comparable for the two quinones (water solubilities of 1.5 and 1.3 mM for DQ and CoQ_1, respectively; log cyclohexane:H_2O partition coefficients 2.45 and 2.65, respectively), but has been attributed instead to steric factors (16, 18). With respect to the relative specificity of NQO1 for the two quinones, although CoQ_1 acts as a substrate for isolated NQO1, a marked preference was observed for DQ as an NQO1 electron acceptor in the intact pulmonary endothelial cells in the present study. This might have been anticipated based on quantitative structure activity studies showing that quinones with van der Waals volume of <200 Å (DQ, 162.9 Å; CoQ1, 243.96 Å) behave as relatively "fast" NQO1 substrates (high K_{cat}/K_m) (1, 41). Thus the basis for the propensity for CoQ_1 to act as an NQO1 substrate in studies of various other cell types is not known and may be attributable in part to species differences in NQO1 electron acceptor preference (17).

CoQ_1 has also been suggested as a TPMET electron acceptor in human red blood cells, Hep G cells, and chick neurons, although whether it is via the same TPMET system that utilizes thiazines (e.g., TBOP) is not known (42, 44). The Hep G and red blood cells carried out both CoQ_1 reduction and CoQ_1H_2 oxidation processes, producing qualitatively similar effects on CoQ_1 extracellular redox status to those seen in the present study (42). However, to the extent that the two studies can be compared given the different experimental conditions, the data suggested a substantially greater net CoQ_1 reduction capacity for the red blood and Hep G cells than for the pulmonary arterial endothelial cells in the present study, implying that the balance between the relative contributions of CoQ_1 reduction and CoQ_1 oxidation reactions that produce the net effect in the extracellular medium is different among the different cell types.

The rotenone-insensitive CoQ_1 reduction mechanism was not identified or characterized other than that it contributed a proportionally greater fraction of the total CoQ_1 reduction capacity for the hyperoxia-exposed than for the normoxic cells and that it did not appear to be NQO1. Given the variety of potential CoQ_1 reductases and the likelihood that expression and/or activity of any given one might also be sensitive to oxidative stress, it is conceivable that a different complement of reductases contributes to the rotenone-insensitive CoQ_1 reduction component in the normoxic and hyperoxia-exposed cells. A difference in the complement of contributing reductases at CoQ_1 concentrations below ~10 μM could also explain the difference in apparent K_m values for normoxic and hyperoxia-exposed cell CoQ_1 reduction (Fig. 5). Of note is that the reduction rates in Fig. 5 were obtained using ferricyanide in the absence of any inhibitors (e.g., rotenone), thereby providing a measure of "net" CoQ_1 reduction that does not reveal the identity or proportional contributions of any contributing quinone reductases.

The deleterious effects of hyperoxia in the lung and pulmonary endothelium are generally accepted to be mediated by production of excessive ROS (19, 39). Recent observations suggest that hyperoxia-induced injury in pulmonary capillary endothelial cells in situ is triggered initially via ROS production at complex I and a relatively

delayed contribution of NADPH oxidase (10). Superoxide formation via complex I has also been associated with development of ischemia-reperfusion injury in the heart and neurodegeneration in Parkinson's disease and other conditions (24, 34). At the same time, complex I is susceptible to ROS-induced inactivation (13). Thus, although on one hand the impact of hyperoxia on complex I may be interpreted as a manifestation of injury, alternatively it might be viewed as an adaptive mechanism, analogous to the association of depressed complex I activity with anesthetic preconditioning for protection from cardiac ischemia-reperfusion injury (38). Insofar as mitochondria-derived ROS have been implicated as signaling molecules in endothelial responses to certain oxidative stresses (e.g., hypoxia and hyperoxia), compromised complex I activity might affect such signaling pathways, since it likely plays a direct or indirect role in mitochondrial ROS generation (10, 35). One might also speculate a potential for secondary effects of altered ROS production on the activity and function of nitric oxide, which has been implicated in regulation of respiration and mitochondrial ROS signaling in vascular endothelium (35).

The pulmonary endothelium encounters various blood borne quinones as environmental, pharmacological, physiological, and dietary components (11). Given its large perfused surface area and its position between the venous and systemic arterial circulations, the pulmonary endothelium has the potential to play a key role in determining the redox status of these substances in the blood, as exemplified by its impact on CoQ_1 in the extracellular medium in the present study. The implication is that for quinones accessible to pulmonary endothelial redox enzymes for which they are substrates, and depending on the tissue permeability of the oxidized and reduced forms, this endothelial function may have an impact on the redox status, and hence bioactivity, of quinones not only in the lung but also in downstream organs. It follows that changes in pulmonary endothelial complex I activity as a result of injury or adaptation may be reflected as alterations in the redox status or disposition of redox active compounds that can permeate the pulmonary endothelial cell membrane and undergo reactions involving complex I. For example, with regard to quinones that may be detoxified by two-electron reduction via complex I, compromised complex I activity may promote generation of the generally more toxic semiquinone. Finally, the study results suggest the potential utility of CoQ_1 as a probe for nondestructive measurements of complex I activity in the intact lung, analogous to the use of DQ for evaluation of lung NQO1 activity.

GRANTS

This research was supported by National Heart, Lung, and Blood Institute Grants R01 HL-65537 and R01 HL-24349 and by the Department of Veterans Affairs.

FOOTNOTES

The costs of publication of this article were defrayed in part by the payment of page charges. The article must therefore be hereby marked "*advertisement*" in accordance with 18 U.S.C. Section 1734 solely to indicate this fact.

AUTHOR NOTES

Address for reprint requests and other correspondence: M. P. Merker, Research Service 151, Zablocki VA Medical Center, 5000 W National Ave., Milwaukee, WI 53295 (e-mail: mmerker@mcw.edu)

REFERENCES

1. Anusevicius Z, Sarlauskas J, Cenas N. Two-electron reduction of quinones by rat liver NAD(P)H:quinone oxidoreductase: quantitative structure-activity relationships. *Arch Biochem Biophys* 404: 254–262, 2002.

2. Audi SH, Bongard RD, Dawson CA, Siegel D, Roerig DL, Merker MP. Duroquinone reduction during passage through the pulmonary circulation. *Am J Physiol Lung Cell Mol Physiol* 285: L1116–L1131, 2003.
3. Audi SH, Bongard RD, Okamoto Y, Merker MP, Roerig DL, Dawson CA. Pulmonary reduction of an intravascular redox polymer. *Am J Physiol Lung Cell Mol Physiol* 280: L1290–L1299, 2001.
4. Audi SH, Zhao H, Bongard RD, Hogg N, Kettenhofen NJ, Kalyanaraman B, Dawson CA, Merker MP. Pulmonary arterial endothelial cells affect the redox status of coenzyme Q0. *Free Radic Biol Med* 34: 892–907, 2003.
5. Audi SH, Bongard RD, Krenz GS, Rickaby DA, Haworth ST, Eisenhauer J, Roerig DL, Merker MP. Effect of chronic hyperoxic exposure on duroquinone reduction in adult rat lungs. *Am J Physiol Lung Cell Mol Physiol* 289: L788–L797, 2005.
6. Barclay AR, Sholler G, Christodolou J, Shun A, Arbuckle S, Dorney S, Stormon MO. Pulmonary hypertension—a new manifestation of mitochondrial disease. *J Inherit Metab Dis* 28: 1081–1089, 2005.
7. Barrientos A, Moraes CT. Titrating the effects of mitochondrial complex I impairment in the cell physiology. *J Biol Chem* 274: 16188–16197, 1999.
8. Beyer RE, Segura-Aguilar J, di Bernardo S, Cavazzoni M, Fato R, Fiorentini D, Galli MC, Setti M, Landi L, Lenaz G. The role of DT-diaphorase in the maintenance of the reduced antioxidant form of coenzyme Q in membrane systems. *Proc Natl Acad Sci USA* 93: 2528–2532, 1996.
9. Bongard RD, Merker MP, Shundo R, Okamoto Y, Roerig DL, Linehan JH, Dawson CA. Reduction of thiazine dyes by bovine pulmonary arterial endothelial cells in culture. *Am J Physiol Lung Cell Mol Physiol* 269: L78–L84, 1995.
10. Brueckl C, Kaestle S, Kerem A, Habazettl H, Krombach F, Kuppe H, Kuebler WM. Hyperoxia-induced reactive oxygen species formation in pulmonary capillary endothelial cells in situ. *Am J Respir Cell Mol Biol* 34: 453–463, 2006.
11. Cadenas E. Antioxidant and prooxidant functions of DT-diaphorase in quinone metabolism. *Biochem Pharmacol* 49: 127–140, 1995.
12. Chan TS, Teng S, Wilson JX, Galati G, Khan S, O'Brien PJ. Coenzyme Q cytoprotective mechanisms for mitochondrial complex I cytopathies involves NAD(P)H: quinone oxidoreductase 1(NQO1). *Free Radic Res* 36: 421–427, 2002.
13. Chen YR, Chen CL, Zhang L, Green-Church KB, Zweier JL. Superoxide generation from mitochondrial NADH dehydrogenase induces selfinactivation with specific protein radical formation. *J Biol Chem* 280: 37339–37348, 2005.
14. Crapo JD, Barry BE, Foscue HA, Shelburne J. Structural and biochemical changes in rat lungs occurring during exposures to lethal and adaptive doses of oxygen. *Am Rev Respir Dis* 122: 123–143, 1980.
15. Dehn DL, Siegel D, Swann E, Moody CJ, Ross D. Biochemical, cytotoxic, and genotoxic effects of ES936, a mechanism-based inhibitor of NAD(P)H:quinone oxidoreductase 1, in cellular systems. *Mol Pharmacol* 64: 714–720, 2003.
16. Di Virgilio F, Azzone GF. Activation of site I redox-driven H_ pump by exogenous quinones in intact mitochondria. *J Biol Chem* 257: 4106–4113, 1982.
17. Faig M, Bianchet MA, Talalay P, Chen S, Winski S, Ross D, Amzel LM. Structures of recombinant human and mouse NAD(P)H:quinone oxidoreductases: species comparison and structural changes with substrate binding and release. *Proc Natl Acad Sci USA* 97: 3177–3182, 2000.
18. Fato R, Estornell E, di Bernardo S, Pallotti F, Parenti CG, Lenaz G. Steady-state kinetics of the reduction of coenzyme Q analogs by complex I (NADH:ubiquinone oxidoreductase) in bovine heart mitochondria and submitochondrial particles. *Biochemistry* 35: 2705–2716, 1996.
19. Freeman BA, Crapo JD. Hyperoxia increases oxygen radical production in rat lungs and lung mitochondria. *J Biol Chem* 256: 10986–10992, 1981.
20. Gardner PR, Nguyen DD, White CW. Aconitase is a sensitive and critical target of oxygen poisoning in cultured mammalian cells and in rat lungs. *Proc Natl Acad Sci USA* 91: 12248–12252, 1994.
21. Genova ML, Bovina C, Marchetti M, Pallotti F, Tietz C, Biagini G, Pugnaloni A, Viticchi C, Gorini A, Villa RF, Lenaz G. Decrease of rotenone inhibition is a sensitive parameter of complex I damage in brain non-synaptic mitochondria of aged rats. *FEBS Lett* 410: 467–469, 1997.

22. Housset B, Junod AF. Effects of culture conditions and hyperoxia on antioxidant enzymes in pig pulmonary artery and aortic endothelium. *Biochim Biophys Acta* 716: 283–289, 1982.
23. Jaiswal AK. Regulation of genes encoding NAD(P)H:quinone oxidoreductases. *Free Radic Biol Med* 29: 254–262, 2000.
24. Jha N, Jurma O, Lalli G, Liu Y, Pettus EH, Greenamyre JT, Liu RM, Forman HJ, Andersen JK. Glutathione depletion in PC12 results in selective inhibition of mitochondrial complex I activity. Implications for Parkinson's disease. *J Biol Chem* 275: 26096–26101, 2000.
25. Kotamraju S, Konorev EA, Joseph J, Kalyanaraman B. Doxorubicininduced apoptosis in endothelial cells and cardiomyocytes is ameliorated by nitrone spin traps and ebselen. Role of reactive oxygen and nitrogen species. *J Biol Chem* 275: 33585–33592, 2000.
26. Lanzillo JJ, Yu FS, Stevens J, Hassoun PM. Determination of xanthine dehydrogenase mRNA by a reverse transcription-coupled competitive quantitative polymerase chain reaction assay: regulation in rat endothelial cells by hypoxia and hyperoxia. *Arch Biochem Biophys* 335: 377–380, 1996.